Chemical Physics Letters 700 (2018) 149–155

Contents lists available at ScienceDirect

Chemical Physics Letters

journal homepage: www.elsevier.com/locate/cplett

Research paper

Quantum chemical approach for condensed-phase thermochemistry (V): Development of rigid-body type harmonic solvation model

Moto Tarumi [a,b], Hiromi Nakai [a,c,d,e,*]

[a] Department of Chemistry and Biochemistry, School of Advanced Science and Engineering, Waseda University, 3-4-1 Okubo, Shinjuku-ku, Tokyo 169-8555, Japan
[b] Advanced Technology Research Laboratories, Nippon Steel & Sumitomo Metal Corporation, 20-1 Shintomi, Futtsu, Chiba 293-8511, Japan
[c] Research Institute for Science and Engineering, Waseda University, 3-4-1 Okubo, Shinjuku-ku, Tokyo 169-8555, Japan
[d] CREST, Japan Science and Technology Agency, Tokyo 102-0075, Japan
[e] Elements Strategy Initiative for Catalysts and Batteries (ESICB), Kyoto University, Katsura, Kyoto 615-8520, Japan

ARTICLE INFO

Article history:
Received 20 December 2017
In final form 3 April 2018
Available online 09 April 2018

Keywords:
Condensed-phase thermochemistry
Quantum chemistry
Harmonic solvation model
Rigid-body approximation
Trouton's rule

ABSTRACT

This letter proposes an approximate treatment of the harmonic solvation model (HSM) assuming the solute to be a rigid body (RB-HSM). The HSM method can appropriately estimate the Gibbs free energy for condensed phases even where an ideal gas model used by standard quantum chemical programs fails. The RB-HSM method eliminates calculations for intra-molecular vibrations in order to reduce the computational costs. Numerical assessments indicated that the RB-HSM method can evaluate entropies and internal energies with the same accuracy as the HSM method but with lower calculation costs.

1. Introduction

Continuum models of solvents, including the polarizable continuum model (PCM), are widely used in quantum chemical calculations to evaluate the reactivity of solutes in liquids [1]. The continuum model takes account of solvent effects and has little computational costs, because only solutes or, in some cases, solutes with neighboring solvents, are treated by quantum mechanics in a cavity, and bulk solvents are described by the continuum around the cavity.

In the quantum chemical treatment of isolated systems, thermodynamic parameters are generally calculated by an ideal gas model (IGM). IGM provides high performance for the evaluation of thermodynamic parameters in gas phases. On the other hand, the calculation of thermodynamic parameters in liquid phases with this continuum model gives unrealistic results due to the overestimation of entropy [2].

Several theoretical models have been developed in order to accurately evaluate thermodynamic parameters in liquid phases. One of the standard methods might be a series of SM*x* models [3–5], which adjusted Gibbs free energies by the parameterization against reference experimental data. For example, SM12 was parameterized over 10 combinations of theoretical levels against 2979 reference experimental data, which include 2503 solvation free energies, 144 transfer free energies of neutral solutes in water and in 90 organic solvents, and 322 solvation free energies of ions in five solvents. Although the SM*x* models can obtain accurate results under the well-parametrized conditions, applicable systems and/or conditions are limited. For example, the temperature dependence of Gibbs free energy is not well demonstrated, because the contributions of enthalpy and entropy are not separated.

The statistic model proposed by Whitesides and coworkers [6] calculates the translational entropy by estimating free volume. Although the interaction between solutes and solvents are not included except for the rigid-body repulsion, the overestimation of translational entropy is reasonably improved. Because the translational entropy is the leading term in the entropy components, the temperature dependence of Gibbs free energy in liquid phase is moderately reproduced. Note that the rotational entropy cannot be estimated by Whitesides' model.

The authors' group has proposed and developed an alternative model, termed by harmonic solvation model (HSM), which combines with the standard polarizable continuum models [2,7–9]. In this model, the interaction between the solute and the cavity, which represents the solvents, is included by the electronic structure calculations. To evaluate the thermodynamic parameters in

* Corresponding author at: Department of Chemistry and Biochemistry, School of Advanced Science and Engineering, Waseda University, 3-4-1 Okubo, Shinjuku-ku, Tokyo 169-8555, Japan.
E-mail address: nakai@waseda.jp (H. Nakai).
URL: http://www.chem.waseda.ac.jp/nakai/ (H. Nakai).

https://doi.org/10.1016/j.cplett.2018.04.006
0009-2614/

liquid phases, the frequency calculation with a Hessian matrix, which is constructed under fixed cavity conditions, is performed. The six lowest frequencies obtained by diagonalizing the Hessian matrix are regarded as the frequencies for the translational and rotational motions of a solute bound by solvents (for linear molecules, the five lowest frequencies are considered). The translational and rotational entropy and internal energy of the solute are estimated by a harmonic oscillator approximation with these frequencies. Note that the lowest six (or five, for linear molecules) modes are discarded in an IGM. We have assessed HSM numerically and showed that it can reproduce experimental trends, including those of boiling points [2], enthalpies of formation and combustion [7], the standard hydrogen electrode potential [8], and solubility [9].

However, HSM calculations by our present program demand high computational costs for large systems because a numerical Hessian with an analytical gradient is adopted, due in large part to the simplicity of the implementation. One of the advantages of a continuum model, namely the low computational cost, has been lost in such implementation. We consider two approaches to solve this problem. One is to implement an analytical Hessian within the framework of HSM. Another approach is to treat translational and rotational motions of solutes, which are distinctive on HSM, separately from intra-molecular vibrations. In this approach, the internal coordinates of a solute molecule are fixed, which means that the solute is approximated as a rigid body. Although the rigid-body approximation results in a disregard of the interaction between the intra-molecular vibration and translation or rotation, the freedom of movement is only six, regardless of the number of atoms constructing the solute molecule. This approach offers the prospect of significant computational cost reduction with a light implementation to existing programs.

In this letter, we propose the second approach, denoted by the rigid-body type harmonic solvation model (RB-HSM), for evaluating the translational and rotational components of entropy and internal energy in solvents. In Section 2, the theoretical aspects of IGM, HSM, and RB-HSM are explained. Section 3 shows computational details. In Section 4, describing the results and discussion, the accuracy of the RB-HSM method is discussed. Application of the results to evaluation of the entropies of vaporization and combustion Gibbs energies are also shown. Finally, conclusions are given in Section 5.

2. Theoretical aspects

2.1. IGM and HSM methods

In the IGM method, which is adopted in standard quantum chemical program packages, the entropies and internal energies for translation, rotation, and vibration are given as follows

$$S^{\mathrm{IGM}}_{\mathrm{trans}} = N_{\mathrm{A}}k_{\mathrm{B}}\left(\frac{3}{2}lnM + \frac{5}{2}lnT - lnP + \mathrm{const.}\right), \tag{1}$$

$$S^{\mathrm{IGM}}_{\mathrm{rot}} = N_{\mathrm{A}}k_{\mathrm{B}}\left(\frac{1}{2}lnABC + \frac{3}{2}lnT - ln\sigma + \mathrm{const.}\right), \tag{2}$$

$$S^{\mathrm{IGM}}_{\mathrm{vib}} = N_{\mathrm{A}}k_{\mathrm{B}}\sum_{i}^{3N-6}\left[\frac{(h\nu_i/k_{\mathrm{B}}T)exp(-h\nu_i/k_{\mathrm{B}}T)}{1-exp(-h\nu_i/k_{\mathrm{B}}T)} - ln\{1-exp(-h\nu_i/k_{\mathrm{B}}T)\}\right], \tag{3}$$

$$E^{\mathrm{IGM}}_{\mathrm{trans/rot}} = \frac{3}{2}N_{\mathrm{A}}k_{\mathrm{B}}T, \tag{4}$$

and

$$E^{\mathrm{IGM}}_{\mathrm{vib}} = N_{\mathrm{A}}k_{\mathrm{B}}T\sum_{i}^{3N-6}\frac{h\nu_i}{k_{\mathrm{B}}T}\left\{\frac{1}{2} + \frac{exp(-h\nu_i/k_{\mathrm{B}}T)}{1-exp(-h\nu_i/k_{\mathrm{B}}T)}\right\}. \tag{5}$$

Here, h, N_{A}, and k_{B} are the Planck, Avogadro, and Boltzmann constants, respectively. P corresponds to the pressure, T the temperature, N the number of atoms, $\{\nu_i\}$ the vibrational frequencies of normal modes, M the total mass, $\{A, B, \text{and } C\}$ the rotational constants, and σ the symmetry number. Note that the six lowest modes corresponding to the translational and rotational motions are neglected because they are treated as the equipartition principle and rigid-rotor approximation in the IGM method.

The HSM method explicitly treats the six lowest modes corresponding to the quasi-translational and quasi-rotational motions that are influenced by solute-solvent interactions as harmonic oscillators [2]. This letter simply describes these modes as translation and rotation. In the HSM method, their entropies and internal energies become as follows:

$$S^{\mathrm{HSM}}_{\mathrm{trans/rot}} = N_{\mathrm{A}}k_{\mathrm{B}}\sum_{i\in\mathrm{trans/rot}}^{3}\left[\frac{(h\nu_i/k_{\mathrm{B}}T)exp(-h\nu_i/k_{\mathrm{B}}T)}{1-exp(-h\nu_i/k_{\mathrm{B}}T)} - ln\{1-exp(-h\nu_i/k_{\mathrm{B}}T)\}\right] \tag{6}$$

and

$$E^{\mathrm{HSM}}_{\mathrm{trans/rot}} = \frac{1}{2}N_{\mathrm{A}}k_{\mathrm{B}}T\sum_{i\in\mathrm{trans/rot}}^{3}\frac{h\nu_i}{k_{\mathrm{B}}T}\left\{\frac{1}{2} + \frac{exp(-h\nu_i/k_{\mathrm{B}}T)}{1-exp(-h\nu_i/k_{\mathrm{B}}T)}\right\}. \tag{7}$$

Note that the formula of $S^{\mathrm{HSM}}_{\mathrm{trans/rot}}$ is identical to that of $S^{\mathrm{IGM}}_{\mathrm{vib}}$, whereas that of $E^{\mathrm{HSM}}_{\mathrm{trans/rot}}$ has a factor of 1/2 to $E^{\mathrm{IGM}}_{\mathrm{vib}}$.

As mentioned above, the treatments of the six lowest modes are different, although both IGM and HSM methods construct a mass-weighted Hessian matrix (i.e. a free constant matrix) of 3 N dimension and diagonalize it to obtain 3 N normal modes. Therefore, the difference in computational cost between the IGM and HSM methods is minor. Strictly, the computation of the force constant matrix in the HSM method is slightly complicated due to the inclusion of the solute-solvent interaction, which is expressed by the interaction between the explicit solute molecule and the cavity of the PCM. Standard quantum chemical programs adopt the analytical Hessian. However, we have used the numerical Hessian with an analytical gradient for the solute-cavity interaction.

2.2. RB-HSM method

The RB-HSM method constructs the following 6-dimensional Hessian matrix of the translations and rotations of a solute in order to calculate only the translational and rotational components of entropy and internal energy.

$$\mathbf{H}^{\mathrm{RB-HSM}} = \begin{pmatrix}
\frac{\partial^2 E}{\partial \widehat{T}_x^{\,2}} & \frac{\partial^2 E}{\partial \widehat{T}_y \partial \widehat{T}_x} & \frac{\partial^2 E}{\partial \widehat{T}_z \partial \widehat{T}_x} & \frac{\partial^2 E}{\partial \widehat{R}_x \partial \widehat{T}_x} & \frac{\partial^2 E}{\partial \widehat{R}_y \partial \widehat{T}_x} & \frac{\partial^2 E}{\partial \widehat{R}_z \partial \widehat{T}_x} \\
\frac{\partial^2 E}{\partial \widehat{T}_x \partial \widehat{T}_y} & \frac{\partial^2 E}{\partial \widehat{T}_y^{\,2}} & \frac{\partial^2 E}{\partial \widehat{T}_y \partial \widehat{T}_z} & \frac{\partial^2 E}{\partial \widehat{R}_x \partial \widehat{T}_y} & \frac{\partial^2 E}{\partial \widehat{R}_y \partial \widehat{T}_y} & \frac{\partial^2 E}{\partial \widehat{R}_z \partial \widehat{T}_y} \\
\frac{\partial^2 E}{\partial \widehat{T}_x \partial \widehat{T}_z} & \frac{\partial^2 E}{\partial \widehat{T}_y \partial \widehat{T}_z} & \frac{\partial^2 E}{\partial \widehat{T}_z^{\,2}} & \frac{\partial^2 E}{\partial \widehat{R}_x \partial \widehat{T}_z} & \frac{\partial^2 E}{\partial \widehat{R}_y \partial \widehat{T}_z} & \frac{\partial^2 E}{\partial \widehat{R}_z \partial \widehat{T}_z} \\
\frac{\partial^2 E}{\partial \widehat{T}_x \partial \widehat{R}_x} & \frac{\partial^2 E}{\partial \widehat{T}_y \partial \widehat{R}_x} & \frac{\partial^2 E}{\partial \widehat{T}_z \partial \widehat{R}_x} & \frac{\partial^2 E}{\partial \widehat{R}_x^{\,2}} & \frac{\partial^2 E}{\partial \widehat{R}_y \partial \widehat{R}_x} & \frac{\partial^2 E}{\partial \widehat{R}_z \partial \widehat{R}_x} \\
\frac{\partial^2 E}{\partial \widehat{T}_x \partial \widehat{R}_y} & \frac{\partial^2 E}{\partial \widehat{T}_y \partial \widehat{R}_y} & \frac{\partial^2 E}{\partial \widehat{T}_y \partial \widehat{R}_z} & \frac{\partial^2 E}{\partial \widehat{R}_x \partial \widehat{R}_y} & \frac{\partial^2 E}{\partial \widehat{R}_y^{\,2}} & \frac{\partial^2 E}{\partial \widehat{R}_z \partial \widehat{R}_y} \\
\frac{\partial^2 E}{\partial \widehat{T}_x \partial \widehat{R}_z} & \frac{\partial^2 E}{\partial \widehat{T}_y \partial \widehat{R}_z} & \frac{\partial^2 E}{\partial \widehat{T}_z \partial \widehat{R}_z} & \frac{\partial^2 E}{\partial \widehat{R}_x \partial \widehat{R}_z} & \frac{\partial^2 E}{\partial \widehat{R}_y \partial \widehat{R}_z} & \frac{\partial^2 E}{\partial \widehat{R}_z^{\,2}}
\end{pmatrix} \tag{8}$$

E is an electronic energy. $\widehat{T}_x$, $\widehat{T}_y$, $\widehat{T}_z$, $\widehat{R}_x$, $\widehat{R}_y$, and $\widehat{R}_z$ are x, y, and z components of translations and rotations of the solute molecule in the rigid-body approximation, respectively. Here, the translations and rotations in the rigid-body approximation signify changes in the

positions of the solute molecule relative to the fixed cavity with constant internal coordinates of the solute molecule. The effect from the solvents to the vibrational parameters, frequency, vibrational entropy, and vibrational energy, is neglected. In this letter, we adopted a numerical Hessian with an analytical gradient **F** due to the simplicity of the implementation. The translational and rotational gradient of a rigid-body molecule are given by

$$\frac{\partial E}{\partial \widehat{T}_x} = -\sum_n^N F_n^x, \quad \frac{\partial E}{\partial \widehat{T}_y} = -\sum_n^N F_n^y, \quad \frac{\partial E}{\partial \widehat{T}_z} = -\sum_n^N F_n^z \tag{9}$$

and

$$\frac{\partial E}{\partial \widehat{R}_x} = -\sum_n^N \frac{r_n^y F_n^z - r_n^z F_n^y}{R^x}, \quad \frac{\partial E}{\partial \widehat{R}_y} = -\sum_n^N \frac{r_n^z F_n^x - r_n^x F_n^z}{R^y}, \quad \frac{\partial E}{\partial \widehat{R}_z} = -\sum_n^N \frac{r_n^x F_n^y - r_n^y F_n^z}{R^z}, \tag{10}$$

where radii of gyrations for x, y, and z axes R^x, R^y, and R^z are given by

$$R^x = \sqrt{\sum_n^N \frac{m_n}{M}\left\{\left(r_n^y\right)^2\right\} + \left\{\left(r_n^z\right)^2\right\}}, \tag{11}$$

$$R^y = \sqrt{\sum_n^N \frac{m_n}{M}\left\{\left(r_n^z\right)^2\right\} + \left\{\left(r_n^x\right)^2\right\}}, \tag{12}$$

and

$$R^z = \sqrt{\sum_n^N \frac{m_n}{M}\left\{\left(r_n^x\right)^2\right\} + \left\{\left(r_n^y\right)^2\right\}}. \tag{13}$$

Here, m_n is the mass of the atom, n and r_n are the coordinates of the atom n when the center of gravity is set to the origin. In order to adjust the dimension in the $\mathbf{H}^{\text{RB-HSM}}$ matrix, a displacement angle of numerical Hessian for rotational motion $\Delta\theta$ is fixed at a quotient of a displacement distance for translational motion Δd divided by a radius of gyration R^x, R^y, or R^z.

The translational and rotational frequencies of the solute are evaluated by the diagonalization of $\mathbf{H}^{\text{RB-HSM}}$. The translational and rotational entropies and internal energies are calculated by Eqs. (6) and (7) with the obtained frequencies. The RB-HSM method requires only 12 evaluations of the gradients for any molecule, whereas the HSM method demands 6 N evaluations. The present method can evaluate translational and rotational thermodynamic parameters more efficiently than the original HSM method in calculations for molecules composed of three or more atoms, and it includes an approximation to separate the translational/rotational motions and internal vibrations.

3. Computational details

We evaluated the entropies of vaporization ΔS_{vap} for seven typical solvents, namely, water (H_2O), methanol (CH_3OH), ethanol (C_2H_5OH), 1,2-dichloroethane (CH_2ClCH_2Cl), benzene (C_6H_6), cyclohexane (C_6H_{12}), and n-heptane (C_7H_{16}). Geometry optimizations were carried out at the second order Møller-Plesset perturbation (MP2) [10] level with a cc-pVTZ basis set [11]. The electronic energy in solution was evaluated by the conductor-like polarizable continuum model (CPCM) [12]. In the CPCM calculations, Bondi's van der Waals radii [13] scaled by α were used. The scale parameter α is set to 1.3 in this letter.

The entropies of vaporization ΔS_{vap} are given by the following equation.

$$\Delta S_{\text{vap}} = S^{\text{gas}} - S^{\text{liq}} = \left(S_{\text{elec}}^{\text{gas}} + S_{\text{vib}}^{\text{gas}} + S_{\text{rot}}^{\text{gas}} + S_{\text{trans}}^{\text{gas}}\right) - \left(S_{\text{elec}}^{\text{liq}} + S_{\text{vib}}^{\text{liq}} + S_{\text{rot}}^{\text{liq}} + S_{\text{trans}}^{\text{liq}}\right) \tag{14}$$

ΔS_{vap} is normally positive because a gas-phase molecule has higher flexibility than a liquid-phase molecule bound to the surroundings. The electronic entropy S_{elec} is zero in the ground electronic state for closed-shell molecules. Because RB-HSM disregards the vibrational entropy, $S_{\text{vib}}^{\text{liq}}$ requires to be estimated by the IGM method. If the change of molecular structure from liquid to gas phase is small, $S_{\text{vib}}^{\text{liq}}$ is close to $S_{\text{vib}}^{\text{gas}}$ in the rigid-body approximation and ΔS_{vap} is approximated by

$$\Delta S_{\text{vap}} = \left(S_{\text{rot}}^{\text{gas}} + S_{\text{trans}}^{\text{gas}}\right) - \left(S_{\text{rot}}^{\text{liq}} + S_{\text{trans}}^{\text{liq}}\right). \tag{15}$$

Eq. (15) does not require to estimate $S_{\text{vib}}^{\text{liq}}$ for the estimation of ΔS_{vap}.

Furthermore, we estimated the combustion Gibbs energies, $\Delta_c G^\circ$ of five organic molecules such as acetonitrile (CH_3CN), acetaldehyde (CH_3CHO), methanol (CH_3OH), benzene (C_6H_6), and ethanol (C_2H_5OH). The combustion Gibbs energies, $\Delta_c G^\circ$ are evaluated by summing up the contributions of energy $\Delta_c E^\circ$, entropy $\Delta_c S^\circ$, and work. The combustion reaction is described as follows:

$$C_{n_C}H_{n_H}N_{n_N}O_{n_O}(\ell) + \frac{4n_C + n_H - 2n_O}{4}O_2(g) \rightarrow n_C CO_2(g) + \frac{n_H}{2}H_2O(\ell) + \frac{n_N}{2}N_2(g), \tag{16}$$

where n_C, n_H, n_N, and n_O mean the numbers of carbon, hydrogen, nitrogen, and oxygen atoms in organic molecules, respectively.

In order to evaluate the electronic energy in the calculations of the combustion energy, we employed the complete-basis-set (CBS) extrapolation. Hartree-Fock (HF) and correlation energies were extrapolated separately. The CBS HF energy $E_{\text{HF}}^{\text{CBS}}$ [14] and CBS correlation energy $E_{\text{corr}}^{\text{CBS}}$ [15,16] were given as follows:

$$E_{\text{HF}}^{\text{CBS}} = E_{\text{HF}}^{\text{X}} - Aexp(-BX) \tag{17}$$

and

$$E_{\text{corr}}^{\text{CBS}} = E_{\text{corr}}^{X} - CX^{-3}. \tag{18}$$

Here, X represents the cardinal number of the Dunning's correlation consistent basis sets. We determined $E_{\text{HF}}^{\text{CBS}}$ as well as parameters A and B in Eq. (17) using the HF energies of the augmented correlation consistent polarized core and valence double-, triple-, and quadruple-zeta (aug-cc-pCVXZ (X = D, T, and Q)) basis sets. $E_{\text{corr}}^{\text{CBS}}$ and parameter C in Eq. (18) were determined by the correlation energy calculated by the coupled cluster with single, double, and non-iterative triple excitations (CCSD(T)) [17] level with aug-cc-pCVXZ (X = T and Q).

All gas-phase calculations were carried out using Gaussian09 [18], and liquid-phase calculations were carried out using Gaussian09 and GAMESS2013 [19]. The HSM and RB-HSM calculations were performed by our original program connected to GAMESS.

4. Results and discussion

4.1. H_2O molecule

Table 1 summarizes the translational, rotational, and vibrational frequencies of a water molecule in gas phase calculated by the IGM method and those in liquid phase calculated by the IGM, RB-HSM, and HSM methods with CPCM under standard conditions (298.15 K and 1 atm). The vibrational frequency is evaluated by all methods except for the RB-HSM method. The translational and rotational frequencies are evaluated by the HSM and RB-HSM methods. The coordinate axes in Table 1 are shown in Fig. 1, and is the optimized structure of the water molecule with the CPCM.

The difference between vibrational frequencies of IGM and HSM indicates the coupling effect between the vibrational motion and the translational/rotational motions. The vibrational frequencies of HSM become lower than those of IGM, followed by the increase in translational and rotational frequencies. The vibrational fre-

Table 1
Translational, rotational, and vibrational frequencies (in cm^{-1}) of a water molecule in gas phase calculated by IGM and those in liquid phase by IGM/CPCM, HSM/CPCM, and RB-HSM/CPCM at the MP2/cc-pVTZ level. *x*, *y*, and *z* axes in translational and rotational modes are described in Fig. 1. δ(H—O—H), ν_s(O—H), and ν_{as}(O—H) represent bending, symmetrical stretching, and asymmetrical stretching modes, respectively.

Phase	Model	Translational			Rotational			Vibrational		
		$\hat{T}_z$	$\hat{T}_x$	$\hat{T}_y$	$\hat{R}_x$	$\hat{R}_y$	$\hat{R}_z$	δ(H—O—H)	ν_s(O—H)	ν_{as}(O—H)
Gas	IGM	–	–	–	–	–	–	1653.68	3852.81	3972.25
Liquid	IGM/CPCM	–	–	–	–	–	–	1642.17	3839.23	3944.77
	RB-HSM/CPCM	63.52	69.55	72.39	148.34	153.67	164.80	–	–	–
	HSM/CPCM	67.61	71.06	73.23	182.18	204.62	208.99	1625.64	3831.18	3933.43
	Δ[a]	(+4.09)	(+1.51)	(+0.84)	(+33.84)	(+50.95)	(+44.19)	(−16.53)	(−8.05)	(−11.34)

[a] For the translation and rotation, the deviations between the HSM/CPCM and RB-HSM/CPCM values are shown in parentheses. For the vibration, the deviations between the HSM/CPCM and IGM/CPCM values are shown in parentheses.

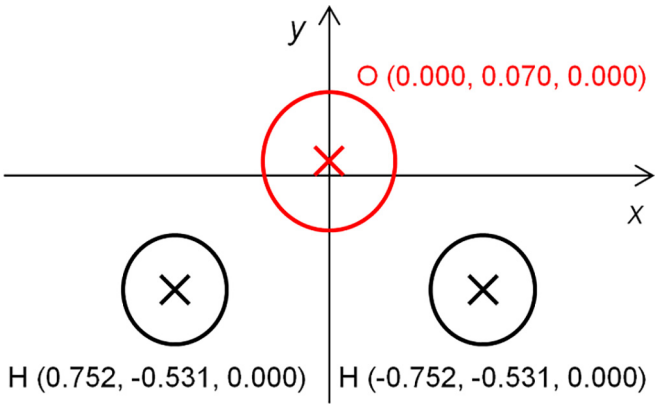

Fig. 1. Coordinates of a water molecule in the *z*-plane optimized by CPCM with the MP2/cc-pVTZ method (in Å).

quencies are indeterminate by RB-HSM because this method fixes bond lengths and angles in the molecule and neglects the intramolecular vibrations. The results of RB-HSM are close to those of HSM in terms of translational and rotational frequencies, although the RB-HSM method gives frequencies that are several dozen cm^{-1} lower than those of HSM owing to the lack of the coupling effect from the vibrational frequency.

Table 2 lists the translational, rotational, and vibrational entropies and internal energies calculated by the gas-phase model, IGM/CPCM, HSM/CPCM, and RB-HSM/CPCM. The entropies and internal energies of IGM are almost equal to those of the gas-phase model, because IGM excludes the restriction from the CPCM solvent. The difference between the entropies of RB-HSM and HSM is 6.49 J/mol/K, which is less than 2 kJ/mol when converted to Gibbs free energy under standard conditions. The internal energy difference between HSM and RB-HSM is 0.1 kJ/mol, which is more trivial than the error in the entropies. The reproduction of HSM by RB-HSM is attributed to the appropriate evaluation of the translational frequencies used to estimate the dominant component of entropy.

The lack of coupling effects between translational/rotational and vibrational frequencies in RB-HSM is considered to cause the slight overestimation of the translational and rotational entropies. On the other hand, the vibrational entropy tends to be underestimated by IGM in the comparison to HSM owing to the lack of coupling effects. The overestimation of translational and rotational entropies in RB-HSM and the underestimation of vibrational entropies in IGM are cancelled mutually when the RB-HSM and IGM methods are used together in order to estimate the total thermodynamic parameters. Like HSM, the combination of RB-HSM and IGM is expected to be a good model for the calculation of total entropies.

4.2. Trouton's rule and its exceptions

Trouton's rule states that the entropy of vaporization at each boiling point is an approximately same value (about 85 J/mol/K) for various compounds [20]. It is well known that the rule has some exceptions, including water, methanol, and ethanol, which are examined in this letter. These exceptions are considered to be caused by the strong electrostatic interactions between molecules.

Table 3 summarizes entropies in gas phase calculated by the IGM method and those in liquid phase by the IGM/CPCM, HSM/CPCM, and RB-HSM/CPCM methods at the boiling points measured experimentally for seven typical solvents. The sum of translational and rotational entropies is shown. In the evaluation of liquid-phase translational and rotational entropies, the RB-HSM method can estimate the results of the HSM method in the range from −4.32 to +8.73 J/mol/K, which is less than 3 kJ/mol in absolute value when converted to Gibbs free energy at each boiling point.

The difference between the RB-HSM and HSM values are negative except for CH_2ClCH_2Cl in Table 3. The coupling between translation/rotation and vibration tends to increase the frequencies of translational/rotational modes and to decrease those of vibrational

Table 2
Translational, rotational, and vibrational entropies (in J/mol/K) and energies (in kJ/mol) of a water molecule in gas phase calculated by IGM and those in liquid phase by IGM/CPCM, HSM/CPCM, and RB-HSM/CPCM at the MP2/cc-pVTZ level under the conditions of 298.15 K and 1 atm.

Phase	Model	Entropy (J/mol/K)			Energy (kJ/mol)		
		S_{trans}	S_{rot}	S_{vib}	E_{trans}	E_{rot}	E_{vib}
Gas	IGM	114.80	49.56	0.03	3.72	3.72	56.70
Liquid	IGM/CPCM	144.80	49.61	0.03	3.72	3.72	56.39
	RB-HSM/CPCM	52.71	32.69	–	3.75	3.89	–
	HSM/CPCM	51.92	26.99	0.10	3.75	3.99	56.17
	Δ[a]	(−0.79)	(−5.70)	(+0.07)	(0.00)	(−0.10)	(−0.22)

[a] For the translation and rotation, the deviations between the HSM/CPCM and RB-HSM/CPCM values are shown in parentheses. For the vibration, the deviations between the HSM/CPCM and IGM/CPCM values are shown in parentheses.

Table 3
Entropies (in J/mol/K) in gas phase calculated by IGM and those in liquid phase by IGM/CPCM, HSM/CPCM, and RB-HSM/CPCM at the MP2/cc-pVTZ level at boiling points. The deviations between the HSM and RB-HSM values are shown in parentheses.

Molecule	Boiling point (K)[a]	Gas phase		Liquid phase					
		$S_{trans+rot}$	S_{vib}	$S_{trans+rot}$				S_{vib}	
		IGM	IGM	IGM/CPCM	RB-HSM/CPCM	HSM/CPCM	Δ	IGM/CPCM	HSM/CPCM
H_2O	373.15	201.82	0.10	201.87	96.35	89.73	(−6.62)	0.11	0.11
CH_3OH	338.15	235.55	8.33	235.59	129.44	122.71	(−6.72)	8.61	10.02
C_2H_5OH	351.45	255.22	25.76	255.26	142.67	137.22	(−5.45)	26.10	28.74
CH_2ClCH_2Cl	356.60	274.88	38.30	274.91	180.69	185.01	(+4.32)	38.69	39.36
C_6H_6	353.25	276.03	28.66	276.04	181.09	172.36	(−8.73)	28.65	28.88
C_6H_{12}	353.85	279.85	51.23	279.85	199.34	197.70	(−1.64)	51.33	51.45
C_7H_{16}	371.60	292.01	146.27	292.01	199.24	198.12	(−1.12)	146.39	148.66

[a] Refs. [20,21].

modes (see Table 1 and Tables S1–S6 in Supporting Information). The HSM method includes this type of coupling effect, whereas the RB-HSM does not. Consequently, the RB-HSM method slightly overestimates translational/rotational entropies in comparison with the HSM method, as seen in Table 2. It should be noted, however, the differences between the RB-HSM and HSM methods are significantly smaller than those between the IGM and HSM methods.

The behavior of CH_2ClCH_2Cl seems exceptional. The frequencies of translational and rotational modes are {16.86, 22.20, 25.91} and {6.40, 11.68, 47.12} in cm^{-1} for RB-HSM, whereas those are {17.03, 22.57, 28.32} and {2.32, 11.62, 69.44} in cm^{-1} for HSM, respectively. The most characteristic mode is the lowest frequency, which does not correspond to translation but to rotation. The coupling with the vibrational motion involved by the HSM method leads to decrease the frequency from 6.40 to 2.32 cm^{-1}. This change might be caused by the weak C-Cl bonding and the heavy Cl atom. In consequence, the decrease of the lowest frequency is the origin of the slight increase of entropy by including the coupling between translation/rotation and vibration by the HSM method.

In view of computational costs, the RB-HSM calculation for C_7H_{16}, which is the largest molecule examined in this letter, is theoretically 11.5 (i.e. a half number of atoms) times as fast as the HSM calculation, because the RB-HSM and HSM methods require 12 and 138 calculations of analytical gradients, respectively.

We calculated ΔS_{vap} by Eqs. (14) and (15) using the value in Table 3. Fig. 2 shows the comparison between experimental [20,21] and calculated ΔS_{vap} at boiling points. As demonstrated by Fig. 2, HSM (green open square) and the combination of RB-HSM and IGM (red plus) could describe experimental trends, including the exceptions of Trouton's rule, whereas IGM (blue cross) failed. The approximation by Eq. (15) (orange open circle) could well reproduce the result by Eq. (14) using RB-HSM and IGM. These results indicate that RB-HSM is useful to estimate entropies for condensed-phase molecules.

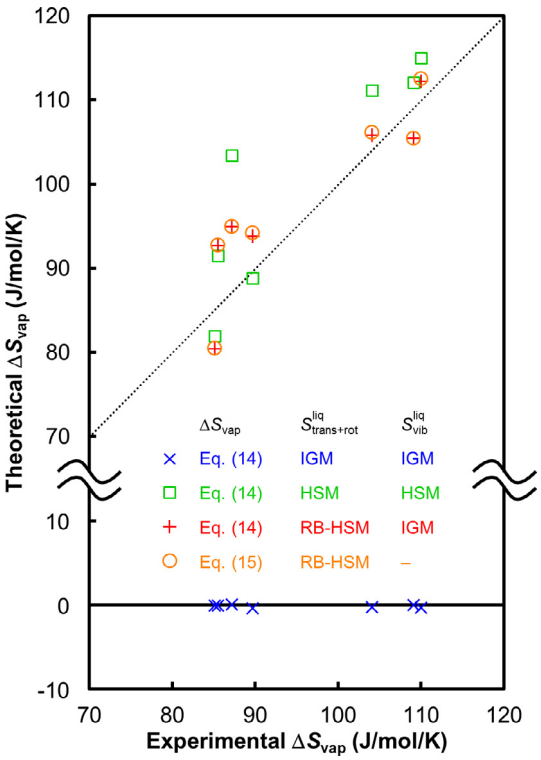

Fig. 2. Comparison between experimental and theoretical entropies of vaporization at boiling points. Blue cross, green open square, and red plus represent the results of Eq. (14) by IGM, HSM, and the combination of RB-HSM and IGM, respectively. Orange open circle represents the results of Eq. (15) by RB-HSM.

4.3. Combustion reaction of organic liquid-phase molecules

Tables 4 and 5 summarize the contributions of entropy $\Delta_c S^\circ$ and energy $\Delta_c E^\circ$ for combustion Gibbs energy under standard conditions. The mean absolute deviations (MAD) of translational and rotational contributions for $\Delta_c S^\circ$ and $\Delta_c E^\circ$ calculated by RB-HSM from those by HSM are 9.65 J/mol/K and 0.37 kJ/mol, respectively. The max absolute deviation of $\Delta_c S^\circ_{trans+rot}$ is 16.36 J/mol/K, which is less than 5 kJ/mol when converted to Gibbs free energy under standard conditions. The deviations of $\Delta_c E^\circ_{trans+rot}$ are further smaller than those of $\Delta_c S^\circ_{trans+rot}$.

Fig. 3 shows the differences between the theoretical and experimental $\Delta_c G^\circ$ and the entropy contribution $T\Delta_c S^\circ$ [22]. As reported in Ref. [7], the errors of the IGM method directly depend on the numbers of liquid-phase molecules in reactants and products, as the following reason. The IGM method tends to greatly overestimate the entropy for a liquid-phase molecule: for example, under the standard condition, the overestimation becomes approximately 30 kJ/mol. However, the overestimation does not change much for molecular species. As a result, such overestimations cancel each other when the numbers of liquid-phase molecules in reactants and products are equal. On the other hand, the cancellation does not happen when the numbers are different.

In Fig. 3, n means the difference of numbers of liquid-phase molecules in reactants and products. As expected, the IGM method systematically increases the error depending on n. On the other hand, both HSM and RB-HSM methods do not show such systematic errors depending on n. MADs of $\Delta_c G^\circ$ calculated by HSM and RB-HSM are 4.03 and 6.53 kJ/mol, respectively. The results indicate that both methods can reasonably estimate the changes of Gibbs energies in the combustion reactions, although RB-HSM tends to give slightly larger errors than HSM.

Table 4
Combustion entropies (in J/mol/K) calculated by IGM/CPCM, HSM/CPSM, and RB-HSM/CPCM with MP2/cc-pVTZ at standard state. The deviations between the HSM and RB-HSM values are shown in parentheses.

Molecule	$\Delta_c S^\circ_{trans+rot}$				$\Delta_c S^\circ_{vib}$	
	IGM/CPCM	RB-HSM/CPCM	HSM/CPCM	Δ	IGM/CPCM	HSM/CPCM
CH_3CN	19.54	−24.37	−30.00	(−5.62)	−3.86	−4.17
CH_3CHO	62.29	−38.77	−46.38	(−7.61)	−9.10	−11.73
CH_3OH	62.59	−40.92	−47.56	(−6.64)	−3.82	−6.46
C_6H_6	89.88	−137.78	−154.14	(−16.36)	−0.60	−0.76
C_2H_5OH	149.58	−58.85	−70.89	(−12.03)	−14.19	−20.07
MAD				9.65		

Table 5
Combustion energies (in kJ/mol) calculated by IGM/CPCM, HSM/CPCM, and RB-HSM/CPCM with MP2/cc-pVTZ at standard state. The deviations between the HSM and RB-HSM values are shown in parentheses.

Molecule	$\Delta_c E^\circ_{trans+rot}$				$\Delta_c E^\circ_{vib}$	
	IGM/CPCM	RB-HSM/CPCM	HSM/CPCM	Δ	IGM	HSM
CH_3CN	2.17	2.62	2.86	(+0.24)	8.11	8.05
CH_3CHO	4.34	4.99	5.32	(+0.33)	2.91	2.60
CH_3OH	4.34	4.96	5.25	(+0.29)	−7.09	−7.26
C_6H_6	5.58	6.61	7.12	(+0.51)	21.26	20.54
C_2H_5OH	8.68	9.68	10.16	(+0.48)	−11.04	−11.44
MAD				0.37		

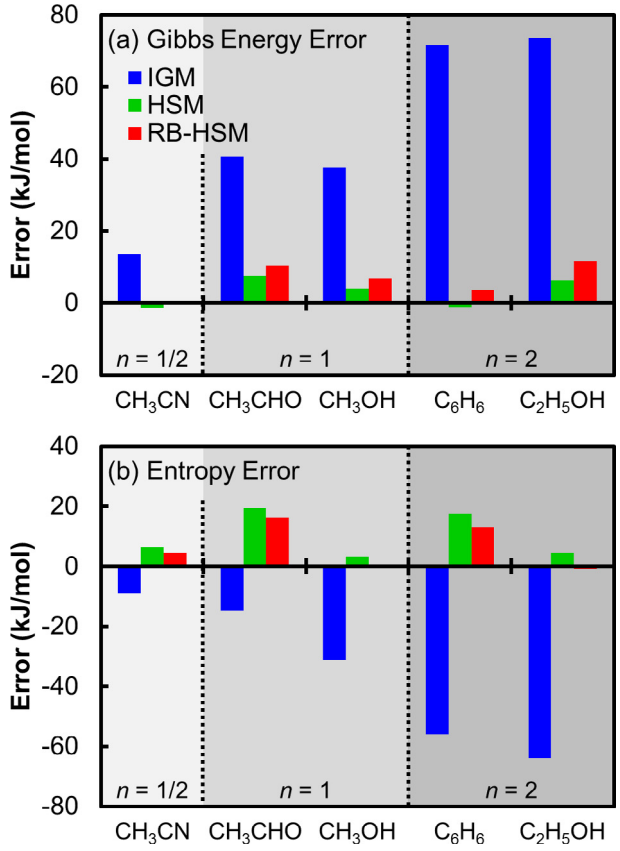

Fig. 3. Errors in theoretical values when compared with experimental results for (a) combustion Gibbs energy and (b) entropy contribution. Blue, green, and red bars represent the results by IGM, HSM, and RB-HSM, respectively. *n* is the difference in the stoichiometric coefficients for the liquid molecules between the two sides of the combustion reactions.

The combination of vibrations described by IGM and translations/rotations described by RB-HSM is superior to HSM from the viewpoint of computational costs. In our previous implementation, HSM needs a 3 *N*-dimensional numerical Hessian calculation. On the other hand, the 3 *N*-dimensional analytical Hessian for IGM is implemented in most of quantum chemical calculation programs. The computational cost of an analytical Hessian is generally lower than that of a numerical Hessian. The combination of IGM and RB-HSM needs a (3*N*-6)-dimensional (or 3 *N*-dimensional) analytical Hessian calculation and a 6-dimensional numerical Hessian calculation. In consequence, the combination of IGM and RB-HSM is significantly faster than HSM to evaluate Gibbs free energies in solution.

5. Conclusions

In this letter, we proposed RB-HSM, which is HSM combined with the rigid-body approximation. This model can estimate translational and rotational frequencies more effectively than HSM using the numerical Hessian with an analytical gradient. The RB-HSM calculation is a half number of atoms times as fast as the HSM calculation, while retaining the same level of accuracy.

We applied the RB-HSM method to calculate the entropies of vaporization at boiling points, which is discussed in Trouton's rule. The experimental trend could be described properly by the RB-HSM method. Furthermore, the RB-HSM method could estimate the combustion Gibbs energy as well as HSM method. These results suggest that the RB-HSM method can be used in the evaluation of thermodynamic parameters for condensed-phase molecules.

In addition, the success of RB-HSM suggests a potential for expansion of HSM. In our previous works as well as in this letter, we have considered only PCM as the solvent model combined with HSM, although essentially, HSM can be teamed with any solvent models. This was caused primarily by the intractable treatment of the interaction between the internal effect of solute-molecular motion and the solute-solvent coupling effect, because these effects are described by different models or computational levels. On the other hand, RB-HSM can consider these effects independently and requires no special treatments. Therefore, RB-HSM is highly suitable for combination with other solvent models.

Acknowledgements

Some calculations were performed at the Research Center for Computational Science (RCCS), Okazaki Research Facilities, and National Institutes of Natural Sciences (NINS). This study was supported in part by the Core Research for Evolutional Science and Technology (CREST) program of the Japan Science and Technology (JST) Agency, Grants-in-Aid for Challenging and Exploratory Research "KAKENHI 15K13629", Strategic Programs for Innovative Research (SPIRE), and Computational Materials Science Initiative (CMSI) of the Ministry of Education, Culture, Sports, Science, and Technology (MEXT), Japan.

Appendix A. Supplementary material

Supplementary data associated with this article can be found, in the online version, at https://doi.org/10.1016/j.cplett.2018.04.006.

References

[1] J. Tomasi, B. Mennucci, R. Cammi, Chem. Rev. 105 (2005) 2999.
[2] H. Nakai, A. Ishikawa, J. Chem. Phys. 141 (2014) 174106.
[3] C.J. Cramer, D.G. Truhlar, Acc. Chem. Res. 41 (2008) 760.
[4] A.V. Marenich, C.J. Cramer, D.G. Truhlar, J. Phys. Chem. B 113 (2009) 6378.
[5] A.V. Marenich, C.J. Cramer, D.G. Truhlar, J. Chem. Theory Comput. 9 (2013) 609.
[6] M. Mammen, E.I. Shakhnovich, J.M. Deutch, G.M. Whitesides, J. Org. Chem. 63 (1998) 3821.
[7] A. Ishikawa, H. Nakai, Chem. Phys. Lett. 624 (2015) 6.
[8] A. Ishikawa, H. Nakai, Chem. Phys. Lett. 650 (2016) 159.
[9] A. Ishikawa, H. Nakai, Chem. Phys. Lett. 655–656 (2016) 103.
[10] M. Head-Gordon, T. Head-Gordon, Chem. Phys. Lett. 220 (1994) 122.
[11] T.H. Dunning Jr., J. Chem. Phys. 90 (1989) 1007.
[12] V. Barone, M. Cossi, J. Phys. Chem. A 102 (1998) 1995.
[13] A. Bondi, J. Phys. Chem. 68 (1964) 441.
[14] A. Halkier, T. Helgaker, P. Jorgensen, W. Klopper, J. Olesen, Chem. Phys. Lett. 302 (1999) 437.
[15] A. Halkier, T. Helgaker, P. Jorgensen, W. Klopper, H. Koch, J. Olsen, A.K. Wilson, Chem. Phys. Lett. 286 (1998) 243.
[16] T. Helgaker, W. Klopper, H. Koch, J. Noga, J. Chem. Phys. 106 (1997) 9639.
[17] G.D. Purvis III, R.J. Bartlett, J. Chem. Phys. 76 (1982) 1910.
[18] M.J. Frisch, G.W. Trucks, H.B. Schlegel, G.E. Scuseria, M.A. Robb, J.R. Cheeseman, G. Scalmani, V. Barone, B. Mennucci, G.A. Petersson, H. Nakatsuji, M. Caricato, X. Li, H.P. Hratchian, A.F. Izmaylov, J. Bloino, G. Zheng, J.L. Sonnenberg, M. Hada, M. Ehara, K. Toyota, R. Fukuda, J. Hasegawa, M. Ishida, T. Nakajima, Y. Honda, O. Kitao, H. Nakai, T. Vreven, J.A. Montgomery Jr., J.E. Peralta, F. Ogliaro, M. Bearpark, J.J. Heyd, E. Brothers, K.N. Kudin, V.N. Staroverov, R. Kobayashi, J. Normand, K. Raghavachari, A. Rendell, J.C. Burant, S.S. Iyengar, J. Tomasi, M. Cossi, N. Rega, J.M. Millam, M. Klene, J.E. Knox, J.B. Cross, V. Bakken, C. Adamo, J. Jaramillo, R. Gomperts, R.E. Stratmann, O. Yazyev, A.J. Austin, R. Cammi, C. Pomelli, J.W. Ochterski, R.L. Martin, K. Morokuma, V.G. Zakrzewski, G.A. Voth, P. Salvador, J.J. Dannenberg, S. Dapprich, A.D. Daniels, Ö. Farkas, J.B. Foresman, J.V. Ortiz, J. Cioslowski, D.J. Fox, Gaussian 09 Revision D.01, Gaussian Inc. Wallingford CT, 2009.
[19] M.W. Schmidt, K.K. Baldridge, J.A. Boatz, S.T. Elbert, M.S. Gordon, J.H. Jensen, S. Koseki, N. Matsunaga, K.A. Nguyen, S. Su, T.L. Windus, M. Dupuis, J.A. Montgomery, J. Comput. Chem. 14 (1993) 1347.
[20] P.W. Atkins, Physical Chemistry, sixth ed., Oxford University Press, 1998.
[21] V. Majer, V. Svodoba, Enthalpies of Vaporization of Organic Compounds: A Critical Review and Data Compilation, Blackwell Scientific Publications, 1985.
[22] CRC Handbook of Chemistry and Physics, 87th ed., CRC Press, Boca Raton, FL, 2006.